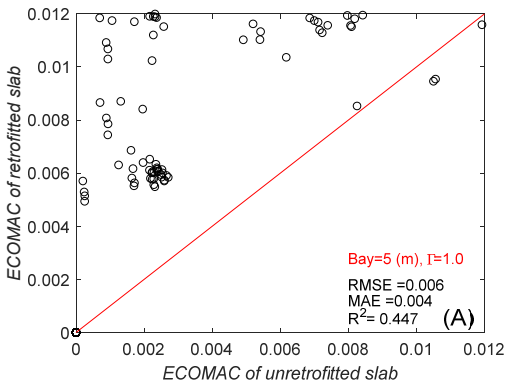

(a) Γ = 1

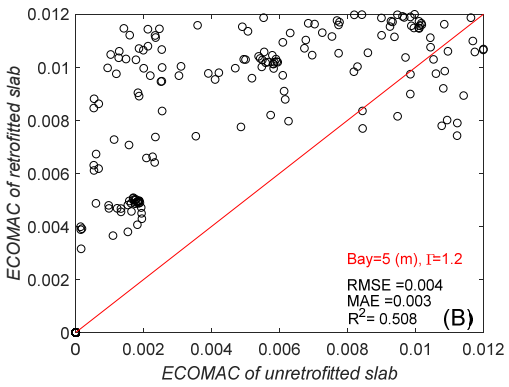

(b) Γ = 1.2

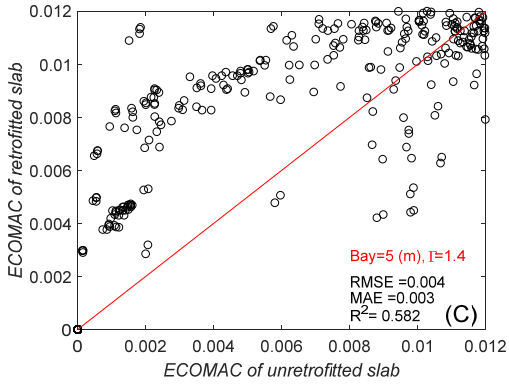

(c) Γ = 1.4

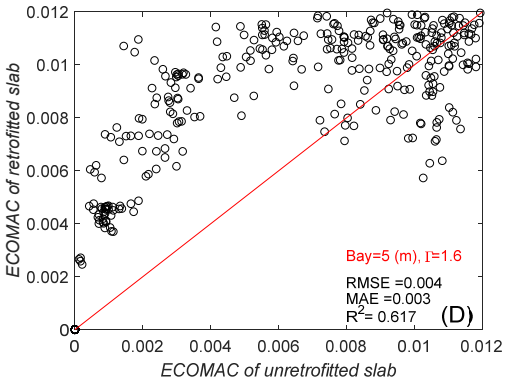

(d) Γ = 1.6

Fig. 15 Comparison the ECOMAC between retrofitted and un-retrofitted slab including various Γ

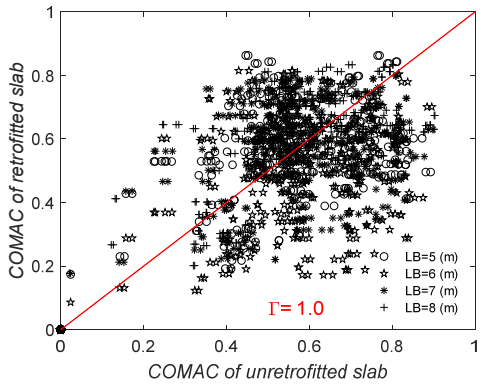

(a) Γ = 1

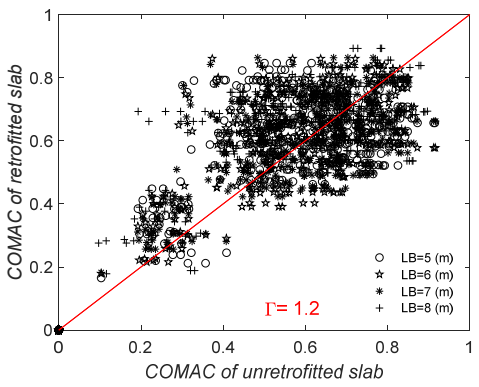

(b) Γ = 1.2

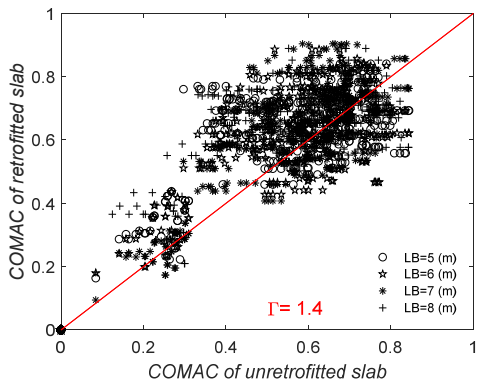

(c) Γ = 1.4

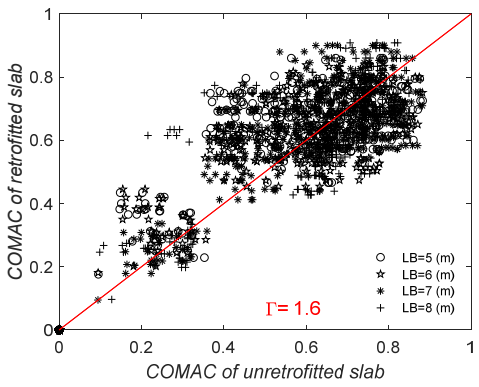

(d) Γ = 1.6

Fig. 16 Comparison the COMAC between retrofitted and un-retrofitted slab

Table 2 The average statistical comparison between retrofitted and un-retrofitted slabs based on COMAC analysis

Γ	MAE	RMSE	R^2
1	0.120	0.164	0.653
1.2	0.099	0.136	0.775
1.4	0.092	0.128	0.816
1.6	0.088	0.120	0.827

Table 3 The average statistical comparison between retrofitted and un-retrofitted slabs based on ECOMAC

Γ	MAE	RMSE	R^2
1	0.002	0.003	0.630
1.2	0.002	0.002	0.709
1.4	0.001	0.002	0.766
1.6	0.001	0.001	0.743

The results of Fig. 14 showed that the comparison of COMAC criteria between retrofitted and un-retrofitted slabs for Γ = 1.0 yielded a high MAE of 0.112, high RMSE of 0.153 and a low R^2 of 0.68. On the other hand, the comparison between them for Γ equal to 1.6 has a low MAE of 0.092, low RMSE of 0.126 and a high R^2 of 0.811. The comprehensive findings suggest that as the slab width increases, the COMAC values for both retrofitted and un-retrofitted items will remain closely comparable, provided that the length of the bay remains constant for all slabs.

Fig. 15 compares the ECOMAC values between retrofitted and un-retrofitted slabs for various amounts of Γ.

The comparison of ECOMAC values between retrofitted and un-retrofitted slabs for various Γ based on Fig. 15 reveals a substantial difference between them. Statistical metrics indicate that for Γ equal to 1, there is a high MAE of 0.004, a high RMSE of 0.006, and a low R^2 of 0.447. The results demonstrate that as the slab width increases, the ECOMAC values for retrofitted and un-retrofitted slabs converge, as long as the bay length remains constant. However, a significant difference between them persists even in this scenario. Therefore, to obtain an accurate solution, the OSP calculated using the ECOMAC approach must consider the different parameters between neighboring elements.

Fig. 16 illustrates the scatter plot of COMAC value between retrofitted and un-retrofitted slabs with varying LB and Γ. This figure encompasses all grids in the case studies, facilitating a comprehensive comparison of the two slab states. Table 2 presents the average statistical comparison of the COMAC for different LBs between the retrofitted and un-retrofitted slab modes. The comparison provides a thorough analysis of the effectiveness of the retrofitting process.

The results of Fig. 16 show that the comparison of COMAC criteria between retrofitted and un-retrofitted slabs for Γ = 1.0 has a highest RMSE of 0.164 and a highest MAE of 0.120 and lowest R^2 of 0.653 between slabs. In

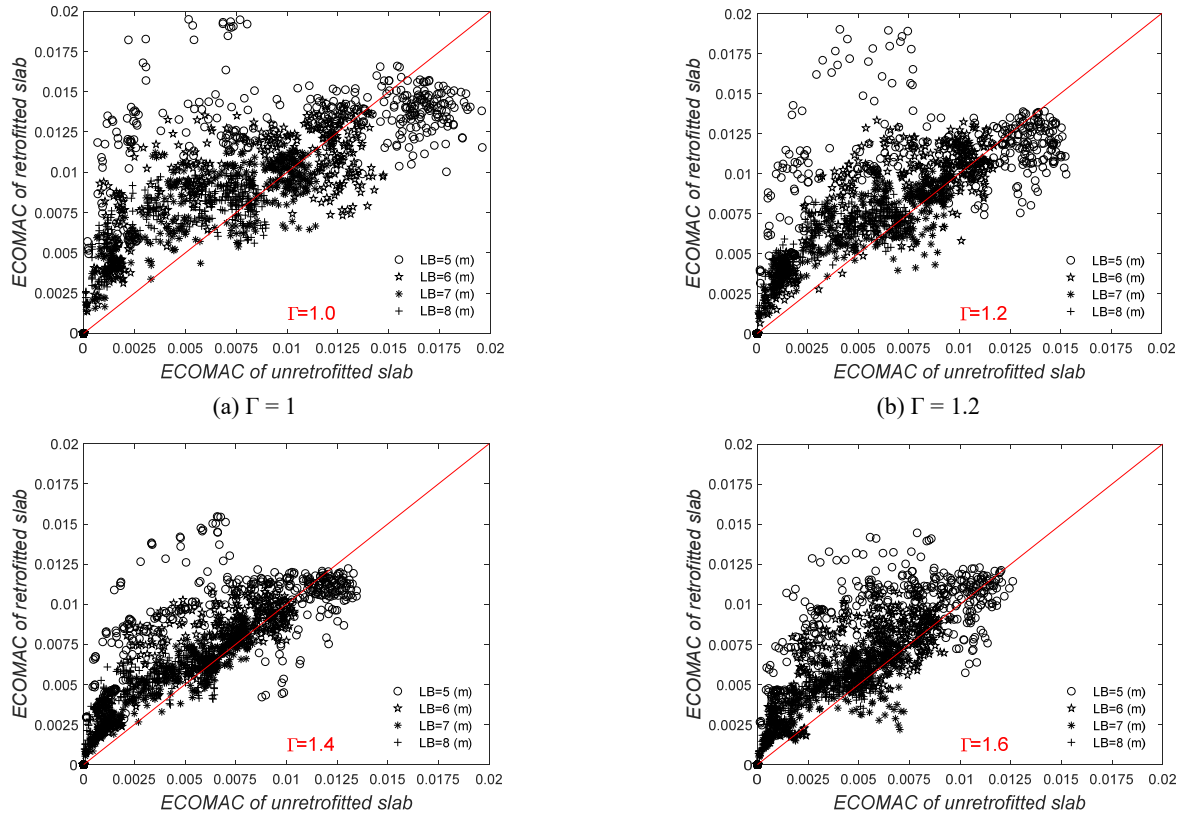

(a) Γ = 1 (b) Γ = 1.2

(c) Γ = 1.4 (d) Γ = 1.6

Fig. 17 Comparison the ECOMAC between retrofitted and un-retrofitted slabs

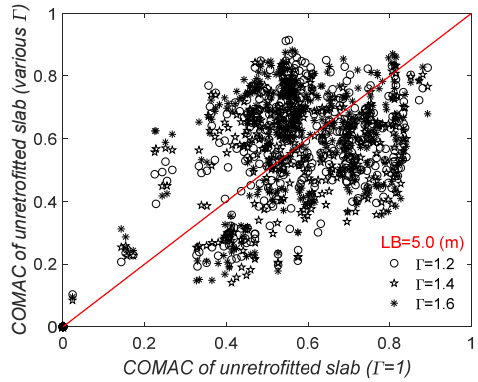

(a) Un-retrofitted slabs

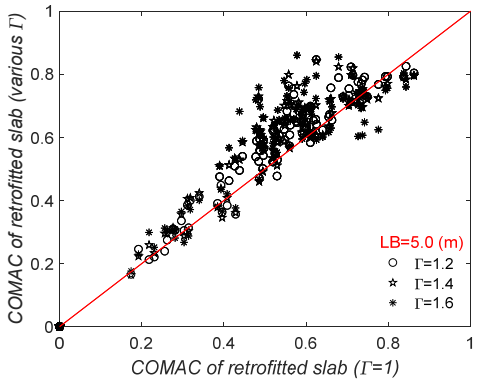

(b) Retrofitted slabs

Fig. 18 Comparison of COMAC sensor location including various Γ for LB = 5

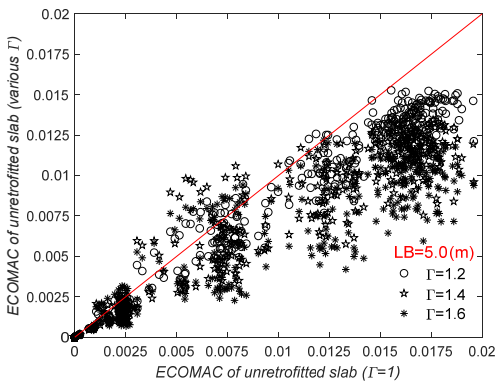

(a) Un-retrofitted slabs

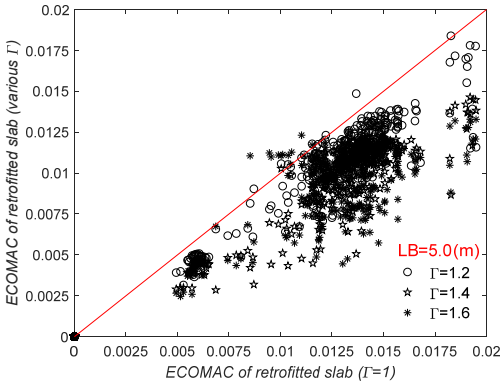

(b) Retrofitted slabs

Fig. 19 Comparison of ECOMAC sensor location including various Γ for LB = 5

Table 4 The statistical comparison between retrofitted and un-retrofitted slabs based on COMAC analysis

Γ	MAE	RMSE	R^2	Slab
1.2	0.046	0.066	0.962	Retrofitted
1.4	0.059	0.082	0.938	Retrofitted
1.6	0.074	0.103	0.897	Retrofitted
1.2	0.132	0.168	0.643	Unretrofitted
1.4	0.127	0.163	0.650	Unretrofitted
1.6	0.136	0.178	0.620	Unretrofitted

Table 5 The statistical comparison between retrofitted slabs based on ECOMAC analysis

Γ	MAE	RMSE	R^2	LB
1.2	0.002	0.002	0.953	Retrofitted
1.4	0.003	0.003	0.929	Retrofitted
1.6	0.003	0.004	0.866	Retrofitted
1.2	0.002	0.002	0.968	Unretrofitted
1.4	0.003	0.004	0.911	Unretrofitted
1.6	0.003	0.005	0.852	Unretrofitted

addition, for Γ = 1.2 the statistical results show that case studies have a high RMSE of 0.136 and a MAE of 0.099 and a low R^2 of 0.775 between slabs. The overall results reveal that with an increase in slab width, the COMAC values for the retrofitted and un-retrofitted slabs tend to converge. Scatter plots of ECOMAC values between retrofitted and un-retrofitted slabs with different LB and Γ are shown in Fig. 17. The average statistical comparison of ECOMAC including different LBs between the two slab modes is given in Table 3.

The results of Fig. 17 and Table 3 indicated that Γ = 1.0 situation, has a high RMSE of 0.003 and a high MAE of 0.002 and a low R^2 of 0.630 among slabs. The outcomes of this figure clearly depict a converging trend in ECOMAC values for both retrofitted and un-retrofitted slabs, as the slab width progressively increases. This tendency is further corroborated by the COMAC results. Fig. 18 compares COMAC values in retrofitted and un-retrofitted slabs with considering various aspect ratios. Table 4 summarizes the statistical differences between retrofitted and un-retrofitted slabs.

The scatter plot depicting COMAC values for retrofitted and un-retrofitted slabs of varying aspect ratios based on Fig. 18 clearly indicates a robust agreement between them. Moreover, there is a low MAE of 0.046 and low RMSE of 0.066 and a high R^2 in average for the retrofitted slabs. These findings are further supported by the statistical analysis presented in Table 4, which highlights the superior

performance of retrofitted slabs compared to un-retrofitted slabs. Fig. 19 compares ECOMAC values in retrofitted and un-retrofitted slabs on various aspect ratios.

Table 5 represents the statistical differences between retrofitted and un-retrofitted slabs. This table shows that there is no significant difference between retrofitted and un-retrofitted slabs based on the ECOMAC analysis. Based on the obtained results, a conclusive inference can be drawn that the retrofitted slab exhibits a significantly lower statistical error rate compared to the un-retrofitted slab. Additionally, the value of R^2 in the retrofitted slab is observed to be substantially higher than that of the un-retrofitted slab. It is also observed that for slabs with larger aspect ratios for spans of 5, 6, 7, and 8 meters, the error rate is comparatively lower, thereby indicating no significant difference between them. The overall findings of the study suggest that the statistical error rate in the COMAC approach is relatively higher than that of the ECOMAC method. However, the difference in the error rates between the two approaches is not significant.

5. Conclusions

The utilization of SHM provides a highly efficient means to ensure the safety of structures. However, this process is limited due to the cost of the sensor system and the coverage intensity of the sensors (Firoozbakht *et al*. 2019), allowing only a restricted number of sensors to be employed. Optimal Sensor Placement (OSP) is crucial for ensuring precise monitoring in terms of both reliability and cost optimization for start-up sensors. Moreover, OSP facilitates the identification of structural vulnerabilities by identifying the most suitable locations for sensor placement. The present study aimed to assess the OSP of retrofitted concrete slabs utilizing NPS. To achieve this objective, the appropriate nonlinear FEM and OSP approach was designed based on the ECOMAC method as a toolbox of MATLAB called the DECOMAC approach, by the authors of this paper. This approach uses distributed ECOMAC analysis instead of line-by-line approach that is evaluated by Ercan and Papadimitriou (2021), Kaveh and Dadras Eslamlou (2019), Tan and Zhang (2020) and Vosoughifar and Manafi (2020). The primary advantage of this innovative approach is its capacity to pinpoint the precise location of sensors by utilizing distributed analysis, in contrast to current methods. The results show that while slab width increases, the COMAC values for the retrofitted and un-retrofitted slabs remain close to each other with respect to the fact that the length of the bay is constant for all slabs. Statistical comparison of DECOMAC criteria between retrofitted and un-retrofitted slabs for aspect ratio 1, shows that there are high values RMSE, MAE and low values R^2 of 0.164, 0.120 and 0.653, respectively. Furthermore, for the aspect ratio 1.2 the statistical results show that that there is a high RMSE, MAE and low R^2 values of 0.136, 0.099 and 0.775, respectively. Therefore, significant differences were observed for statistical errors and R^2 between aspect ratios 1 and 1.2 compared to other ratios.

The results indicated that the ECOMAC values for retrofitted and un-retrofitted slabs remain close to each other while the slab width increases. It can be inferred that the statistical error rate associated with the COMAC and ECOMAC methods is higher compared to the DECOMAC approach, which means that the DECOMAC method performs better in the OSP of slabs. Thus, the modified DECOMAC approach can detect the problems of OSP more accurately than the current COMAC and COMAC methods. Therefore, the OSP obtained using the DECOMAC method is a better solution due to the simultaneous consideration of adjacent elements according to the distributed method. As a consequence, both designers and owners of concrete slabs should regard the DECOMAC method as a viable option to accurately determine the sensor location's effectiveness.

This study focused on the importance of SHM of two-way reinforced concrete slabs using NPS as external reinforcement. The MATLAB toolbox named DECOMAC was developed to optimize the process of sensor placement using a nonlinear FEM approach and a multi-objective function based on the distributed ECOMAC method. The study considered case studies of concrete slabs with different aspect ratios and found that the optimized sensor placement by the DECOMAC algorithm showed a significant difference between un-retrofitted and retrofitted slabs.

References

ACI 318 (2014), Building Code Requirements for Reinforced Concrete and Commentary, American Concrete Institute, ACI Committee 318; Farmington Hills, IL, USA, 348.

Afefy, H.M., Baraghith, A.T and Mahmoud, M.H. (2019), "Retrofitting of defected reinforced-concrete cantilever slabs using different techniques", *Mag. Concr. Res.*, **72**(14), 703-719. https://doi.org/10.1680/jmacr.18.00340

Bekas, D., Grammatikos, S.A., Kouimtzi, C. and Paipetis, A.S. (2015), "Linear and non-linear electrical dependency of carbon nanotube reinforced composites to internal damage", *IOP Conference Series: Materials Science and Engineering*. https://doi.org/10.1088/1757-899X/74/1/012002

Coppolino, R.N. and Rubin, S. (1980), "Detectability of structural failures in offshore platforms by ambient vibration monitoring", *Proceedings of the 12th Annual Offshore Technology Conference*, pp. 101-110.

Ercan, T. and Papadimitriou, C. (2021), "Optimal sensor placement for reliable virtual sensing using modal expansion and information theory", *Sensors*, **21**(10), 3400. https://doi.org/10.3390/s21103400

Eringen, A.C. and Edelen, D.G.B. (1972), "On nonlocal elasticity", *Int. J. Eng. Sci.*, **10**, 233-248. https://doi.org/10.1016/0020-7225(72)90039-0

Fernandes, H., Lúcio, V. and Ramos, A. (2017), "Strengthening of RC slabs with reinforced concrete overlay on the tensile face", *Eng. Struct.*, **132**, 540-550. https://doi.org/10.1016/j.engstruct.2016.10.011

Firoozbakht, M., Vosoughifar, H. and Ghari Ghoran, A. (2019), "Coverage intensity of optimal sensors for common, isolated, and integrated steel structures using novel approach of FEM-MAC-TTFD", *Int. J. Distrib. Sens. Netw.* https://doi.org/10.1177/1550147719857568

Guo, Z., Xu, Z. and Chen, C. (2017), "Behavior of GFRP retrofitted reinforced concrete slabs subjected to conventional explosive blast", *Mater. Struct.*, **50**, 236. https://doi.org/10.1617/s11527-017-1107-6

Herraiz, B. and Vogel, T. (2016), "Novel design approach for the

analysis of laterally unrestrained reinforced concrete slabs considering membrane action", *Eng. Struct.*, **123**, 313-329. https://doi.org/10.1016/j.engstruct.2016.05.033

Hunt, D.L., Weiss, S.P., West, W.M., Dunlap, T.A. and Freemeyer, S.R. (1990), "Development and implementation of a shuttle modal inspection system", *Sound Vib.*

Kang, I., Schulz, M.J., Kim, J.H., Shanov, V. and Shi, D. (2006), "A carbon nanotube strain sensor for structural health monitoring", *Smart Mater. Struct.*, **15**, 737. https://doi.org/10.1088/0964-1726/15/3/009

Kaveh, A., Talaei, A.S. and Nasrollahi, A. (2016), "Application of Probabilistic Particle Swarm in Optimal Design of Large-Span Prestressed Concrete Slabs", *Iran. J. Sci. Technol. Trans. Civil Eng.*, **40**, 33-40. https://doi.org/10.1007/s40996-016-0005-4

Kaveh, A. and Dadras Eslamlou, A. (2019), "An efficient two-stage method for optimal sensor placement using graph-theoretical partitioning and evolutionary algorithms", *Struct. Health Monit.*, **26**, e2325. https://doi.org/10.1002/stc.2325

Kaveh, A., Dadras Eslamlou, A., Rahmani, P. and Amirsoleimani, P. (2022), "Optimal sensor placement in large-scale dome trusses via Q-learning-based water strider algorithm", *Struct. Control Health Monit.*, **29**(7), e2949. https://doi.org/10.1002/stc.2949

Khajehdehi, R. and Panahshahi, N. (2016), "Effect of openings on in-plane structural behavior of reinforced concrete floor slabs", *J. Build. Eng.*, **7**, 1-11. https://doi.org/10.1016/j.jobe.2016.04.011

Konka, H.P., Wahab, M.A. and Lian, K. (2013), "Piezoelectric fiber composite transducers for health monitoring in composite structures", *Sens. Actuator A Phys.*, **194**, 84-94. https://doi.org/10.1016/j.sna.2012.12.039

Lu, S., Tian, C., Wang, X., Zhang, L., Du, K., Ma, K. and Xu, T. (2018), "Strain sensing behaviors of GnPs/epoxy sensor and health monitoring for composite materials under monotonic tensile and cyclic deformation", *Compos. Sci. Technol.*, **158**, 94-100. https://doi.org/10.1016/j.compscitech.2018.02.017

Ma, C., Wang, D. and Wang, Z. (2017), "Seismic retrofitting of full-scale RC interior beam-column-slab subassemblies with CFRP wraps", *Compos. Struct.*, **159**, 397-409. https://doi.org/10.1016/j.compstruct.2016.09.094

Maheri, M.R., Khajeheian, M.K. and Vatanpour, F. (2019), "In-plane seismic retrofitting of hollow concrete block masonry walls with RC layers", *Structures*, **20**, 425-436. https://doi.org/10.1016/j.istruc.2019.05.008

Mosalam, K.M. and Mosallam, A.S. (2001), "Nonlinear transient analysis of reinforced concrete slabs subjected to blast loading and retrofitted with CFRP composites", *Compos. B. Eng.*, **32**(8), 623-636. https://doi.org/10.1016/S1359-8368(01)00044-0

Navarro, M., Ivorra, S. and Varona, F.B. (2018), "Parametric computational analysis for punching shear in RC slabs", *Eng. Struct.*, **165**, 254-263. https://doi.org/10.1016/j.engstruct.2018.03.035

Sengezer, E. and Seidel, G. (2017), "Structural Health Monitoring of Nanocomposite Bonded Energetic Materials Through Piezoresistive Response", *AIAA J.*, **56**, 1-14. https://doi.org/10.2514/1.J056178

Shokouhi, S.K. and Vosoughifar, H. (2013), "Optimal sensor placement in the lightweight steel framing structures using the novel TTFD approach subjected to near-fault earthquakes", *J. Civil Struct. Health Monit.*, **3**, 257-267. https://doi.org/10.1007/s13349-013-0053-4

Tan, Y. and Zhang, L. (2020), "Computational methodologies for optimal sensor placement in structural health monitoring: A review", *Struct. Health Monit.*, **19**(4), 1287-1308. https://doi.org/10.1177/1475921719877579

Tan, A.C., Cha, J.J.Y. and Kang, I. (2011), "Novel corrosion sensor based on carbon nanotube composites for structural health monitoring", *Proceedings of the Thermal and Materials Nanoscience and Nanotechnology for Structural Health Monitoring*, Antalya, Turkey, Begell House, pp. 1-7. http://dx.doi.org/10.1615/ICHMT.2011.TMNN-2011.70

Thiagarajan, G., Kadambi, A.V., Robert, S. and Johnson, C.F. (2015), "Experimental and finite element analysis of doubly reinforced concrete slabs subjected to blast loads", *Int. J. Impact Eng.*, **75**, 162-173. https://doi.org/10.1016/j.ijimpeng.2014.07.018

Vandiver, J.K. (1977), "Detection of structural failure on fixed platforms by measurement of dynamic response", *J. Pet. Technol.*, 305-310. https://doi.org/10.4043/2267-MS

Vosoughifar, H. and Khorani, M. (2019), "Optimal Sensor Placement of RCC Dam using Modified Approach of COMAC-TTFD", *KSCE J. Civil Eng.*, **23**, 2933-2947. https://doi.org/10.1007/s12205-019-0716-8

Vosoughifar, H. and Manafi, P. (2020), "Sensor location in concrete slabs with various layout of opening using modified 'FEMS-COMAC' approach", *Earthq. Eng. Eng. Vib.*, **19**, 205-222. https://doi.org/10.1007/s11803-020-0557-y

Vosoughifar, H., Shokouhi, S.K. and Farshadmanesh, P. (2012), "Optimal sensor placement of steel structure with UBF system for SHM using hybrid FEM-GA technique", *Civil Structural Health Monitoring Workshop*. http://creativecommons.org/licenses/by/3.0/

Wang, W. (2013), "Towards structural health monitoring in carbon nanotube reinforced composites", Bachelor's Thesis; Massachusetts Institute of Technology, Department of Materials Science and Engineering.

Wang, G., Wang, Y., Zhang, P., Zhai, Y., Luo, Y., Li, L. and Luo, S. (2018), "Structure dependent properties of carbon nanomaterials enabled fiber sensors for in situ monitoring of composites", *Compos. Struct.*, **195**, 36-44. https://doi.org/10.1016/j.compstruct.2018.04.052

Yi, T.H., Zhou, G.D., Li, H.N. and Wang, C.W. (2016), "Optimal placement of triaxial sensors for modal identification using hierarchic wolf algorithm", *Struct. Health Monit.*, **24**(8). https://doi.org/10.1002/stc.1958

HJ